Published in final edited form as:
J Immunol. 2014 February 15; 192(4): 1630–1640. doi:10.4049/jimmunol.1302743.

Intradermal delivery of *Shigella* IpaB and IpaD type III secretion proteins: Kinetics of cell recruitment and antigen uptake, mucosal and systemic immunity, and protection across serotypes

Shannon J. Heine[*], **Jovita Diaz-McNair**[*], **Abhay U. Andar**[†], **Cinthia B. Drachenberg**[‡], **Lillian van de Verg**[§], **Richard Walker**[§], **Wendy L. Picking**[¶], and **Marcela F. Pasetti**[*]

[*]Center for Vaccine Development and Department of Pediatrics, University of Maryland School of Medicine, Baltimore, MD

[†]Pharmaceutical Sciences Department, University of Maryland School of Pharmacy, Baltimore, MD

[‡]Department of Pathology, University of Maryland School of Medicine, Baltimore, MD

[§]Enteric Vaccine Initiative, PATH, Washington, DC

[¶]Department of Microbiology and Molecular Genetics, Oklahoma State University, Stillwater, OK

Abstract

Shigella is one of the leading pathogens contributing to the vast pediatric diarrheal disease burden in low-income countries. No licensed vaccine is available and the existing candidates are only partially effective and serotype-specific. *Shigella* type III secretion system proteins IpaB and IpaD, which are conserved across *Shigella* spp., are candidates for a broadly protective, subunit-based vaccine. Herein, we investigated the immunogenicity and protective efficacy of IpaB and IpaD administered intradermally (i.d.) with a double-mutant of the *E. coli* heat-labile enterotoxin (dmLT) adjuvant using microneedles. Different dosage levels of IpaB and IpaD with or without dmLT were tested in mice. Vaccine delivery into the dermis, recruitment of neutrophils, macrophages, dendritic cells (DC) and Langerhans cells (LC), and colocalization of vaccine antigens within skin-activated antigen presenting cells (APC) was demonstrated through histology and immunofluorescence microscopy. Ag-loaded neutrophils, macrophages, DC and LC remained in the tissue at least one week. IpaB, IpaD and dmLT-specific serum IgG and IgG secreting cells were produced following i.d. immunization. The protective efficacy was 70% against *S. flexneri* and 50% against *S. sonnei*. Similar results were obtained when the vaccine was administered intranasally, with the i.d. route requiring 25-40 times lower doses. Distinctively, IgG was detected in mucosal secretions; sIgA as well as mucosal and systemic IgA antibody secreting cells (ASC) were seemingly absent. Vaccine-induced T cells produced IFN-γ, IL-2, TNF-α, IL-17, IL-4, IL-5 and IL-10. These results demonstrate the potential of i.d. vaccination with IpaB and IpaD to prevent *Shigella* infection and support further studies in humans.

Correspondence: Marcela F. Pasetti; University of Maryland, Center for Vaccine Development, 685 West Baltimore St., Baltimore, MD 21201; Fax: 410-706-6205; Tel: 410-706-2341; mpasetti@medicine.umaryland.edu.

The authors declare no conflicts of interest for the work presented herein.

Keywords

Shigella vaccines; intradermal vaccination; dendritic cells

Introduction

Shigella spp. are among the handful of enteric pathogens that account for most of the cases of diarrhea in children under five years of age in sub-Saharan Africa and south Asia (1). Even if mortality is averted, the disease leads to impaired health and quality of life, particularly if acquired at an early age (2,3). Despite the long-standing interest in control measures, no commercial vaccine is currently available. To be used globally, a vaccine would need to prevent infection caused by *S. dysenteriae* 1 (which causes epidemic dysentery), *S. sonnei* (affecting mostly travelers and daycare centers), and all 16 *S. flexneri* serotypes (mostly responsible for endemic disease) (4). Efforts to develop an effective vaccine have produced several candidates, some of which have been tested in human clinical trials with promising results [Reviewed in (5-8)]. Most of these vaccines, however, are serotype-specific and therefore their protective capacity is limited to the serotype from which they were derived. In the pursuit of a broad-spectrum prophylactic intervention, we have proposed the use of *Shigella* type III secretion system (TTSS) proteins IpaB and IpaD, which are highly conserved among *Shigella* serotypes, as components of a subunit-based broad protective vaccine. These proteins have an essential role in pathogenesis as they participate in the assembly of the TTSS needle tip complex, which creates a pore in the host cell membrane and allows the translocation of bacterial effector proteins that ultimately lead to cell death (9,10). Individuals living in endemic areas who are constantly exposed to the organism develop antibodies against *Shigella* O antigen (11) and Ipas (12,13), both of which are believed to contribute to naturally acquired protective immunity (5). An association has been described between the levels of IpaB-specific serum IgG and IgA B memory cells and reduced severity of disease upon experimental challenge in human adult volunteers pre-exposed to live vaccine organisms or wild type *Shigella* (14). In pre-clinical studies, mucosally delivered IpaB and IpaD have been shown to protect against lethal pulmonary *Shigella* infection in mice (15,16).

Given that *Shigella* is an enteric pathogen, oral immunization with candidate vaccines would seem the most practical approach to induce mucosal immunity that could block and prevent the organism from breaching the intestinal barrier. Disappointingly, the success of oral vaccination has been elusive. Routine vaccines have been less immunogenic when administered orally to children living in developing countries, compared with industrialized nations. This has been attributed to multiple natural barriers that interfere with immunological priming in the gut (17,18). In animal studies, orally delivered IpaB and IpaD failed to induce substantial protection, while vigorously immunogenic and fully protective when given intranasally (i.n.).

Intradermal immunization using improved injection devices has gained attention as a safe, practical and effective strategy to enhance vaccine immunogenicity (19). Because of its simplicity and efficiency, this mode of vaccination is particularly attractive for use in

children. The feasibility of this approach has been demonstrated by the successful administration of the *Mycobacterium bovis* bacillus Calmette-Guerin (BCG) to millions of newborns and infants throughout the world. Multiple human clinical studies have shown successful immunization against influenza, rabies, polio, hepatitis and other pathogens through i.d. delivery of commercial vaccines (19-21). Intradermal vaccination against seasonal influenza using microneedles has been approved in Europe since 2009 (22) and in the US since 2011 (19,23). Vaccination via the i.d. route is simple and extremely efficient, requiring a fraction of the dosage typically given intramuscularly or subcutaneously (24). Its success has been attributed to the abundant number of specialized APC (i.e., DC and LC) residing in the dermis and adjacent epidermal layer, which capture vaccine antigens in their proximity, process and transport them to the draining lymph nodes (DLN) for presentation and stimulation of T cells (25). Vaccine Ag that reach the DLN also activate B cells. DC activated in the skin prime $CD4^+$ and $CD8^+$ effector and central memory T cells. Central memory T cells recirculate, may become activated outside the DLN and potentially migrate to effector sites (25). Particularly relevant for clearance of *Shigella* would be the induction of IFN-γ-secreting $CD4^+$ T cells as well as ASC producing high-avidity antibodies that could mediate microbial exclusion and phagocytic killing (5).

In this study, we investigated the early immunological events associated with i.d. immunization with *Shigella* IpaB and IpaD that lead to immunological priming. In particular, we examined the recruitment of immune cells to the injection site and adjacent tissues as well as antigen uptake and activation of skin APC. We also fully characterized the immune responses induced in the systemic and mucosal compartments and the protective efficacy of this vaccine against different *Shigella* serotypes.

Materials and Methods

Vaccine components

The *E. coli* double mutant heat-labile toxin [LT (R192G/L211A) or dmLT] was produced at the Walter Reed Army Institute of Research following previously described affinity chromatography methods (26) and obtained through PATH. Recombinant IpaB complexed with the chaperone IpgC (IpaB/IpgC) and IpaD were also purified via affinity and size-exclusion chromatography (27), and quantified using 280nm extinction coefficients (28). To obtain IpaB for immunological assays and for use as vaccine, IpaB/IpgC was treated with with-Octyl-oligo-oxyethylene (OPOE) to release the IpgC chaperone.

Mice, vaccination and experimental infection with virulent organisms

Female BALB/c mice (7-8 weeks old, Charles River Laboratories, Wilmington, MA) were immunized i.d. by delivering a 25 μl volume of inoculum into the upper right thigh (shaved the day before), using the NanoPass MicronJet 600 needle (NanoPass Technologies Ltd., Nes Ziona, Israel) attached to a 250 μl Hamilton 700 Series Microliter Syringe (Hamilton Company, Reno, NV). The microneedles were inserted into the bare skin at a 45-degree angle, locked in that position, and the inoculum was delivered slowly monitoring the proper formation of a bleb; the needles were kept in place for five seconds before removal. Three dosage levels of IpaB/IpgC and IpaD were tested in the first experiment: 1) 50 ng of IpaB/

IpgC and 100 ng of IpaD (referred to as the “low” dose); 2) 100 ng of IpaB/IpgC and 250 ng of IpaD (referred to as the “medium” dose); and 3) 200 ng of IpaB/IpgC and 500 ng of IpaD (referred to as the “high” dose). In all instances, 100 ng of *E. coli* dmLT was added as adjuvant. The medium and high doses, which proved the most immunogenic in the first experiment, were included in a second experiment with and without adjuvant. A group immunized i.n. with 2.5 μg of IpaB/IpgC or IpaB, 10 μg of IpaD, and 2.5 μg of *E. coli* dmLT, known to generate potent responses (15,16), was included as positive control in both experiments. Intranasal vaccination was performed by dispensing 30 μl of inoculum (15 μl into each nare) with a pipette, as previously described (15,16). Negative control groups received 100 ng of dmLT or PBS i.d. All groups were vaccinated on days 0, 14 and 28. Serum samples, fecal extracts and bronchoalveolar lavage fluid (BALF) from individual animals were prepared as previously described (15,16). On day 56 after vaccination, mice were challenged i.n. with 5.4×10^7 to 5.8×10^7 CFU of *S. flexneri* 2a 2457T or with 1.35×10^8 CFU of *S. sonnei* 53G (15,16); the doses used correspond to ~10 MLD_{50} for each organism, and both are human virulent strains. All animal studies and procedures were approved by the University of Maryland School of Medicine Institutional Animal Care and Use Committee.

Antibodies, Ab-secreting cells (ASC) and cytokines

Antibodies specific for IpaB, IpaD and dmLT were measured in serum, stool and mucosal lavages by ELISA as previously described (15,16). For IgG subclass assays, HRP-labeled anti-mouse IgG1 and IgG2a (Southern Biotech, Birmingham, AL) were used as detection conjugates. The frequency of IgG and IgA ASC in the lungs, spleens and bone marrow were measured by ELISpot, as described before (15,16). Cytokine levels were measured in culture supernatants of spleen cells (2×10^5 in 100 μl) stimulated for 48 h with 10 μg/ml of IpaB and IpaD, using the MSD Mouse TH1/TH2 9-Plex and IL-17 Ultra-Sensitive Kits (Meso Scale Discovery, Gaithersburg, MD) (16).

Histology immunohistochemistry and confocal immunofluorescence

To confirm proper i.d. delivery and to track tissue distribution of the inoculum, mice were injected i.d. with India ink (10% in PBS) and euthanized at 4 h, 24 h and 1 wk after injection. Skin and muscle tissue were removed, embedded in paraffin and sliced into 5 μm thick sections. The slides were then stained with H&E and 2× and 40× tissue images were captured using an Olympus BH-2 microscope with an SPOT 4 Mega Pixel RT color camera and imaging software to visualize overall distribution of the dye and cellular inflammatory infiltration at the injection site. For immunohistochemistry (IHC) and immunofluorescence (IF) staining, mice were injected i.d. with IpaB, IpaD and dmLT (medium dosage level described above) and euthanized 4 h, 24 h and 1 wk after injection. Mice injected i.d. with PBS and euthanized 30 minutes after injection served as negative controls. Skin tissue, including the site of injection and surrounding areas, was removed, sectioned, embedded in Tissue-Tek Optimal Cutting Temperature compound (Sakura, The Netherlands) and flash frozen in 2-Methylbutane contained in liquid nitrogen. Five μm frozen tissue sections were prepared and fixed with cold acetone for staining. For IHC, slides were washed in PBS and immersed in PBS/0.3% H_2O_2 to exhaust endogenous peroxidase activity. The tissue sections were blocked with 10% rabbit serum and stained with anti-CD4 (clone: RM4-5) and anti-

CD8α (clone: 53-6.7) (BD Biosciences, San Jose, CA), anti-CD207 (Langerin) (clone: eBioL31) (eBioscience, San Diego, CA) and anti-macrophage specific lectin antibody (clone: ER-MP23) (Abcam, Cambridge, MA). Slides were then washed and biotinylated rabbit anti-rat (Molecular Probes-Invitrogen, Grand Island, NY) was added as secondary Ab. Sections stained by IHC with anti-CD11c (BD Biosciences, San Jose, CA) were blocked with 10% goat serum before incubation with primary antibodies, then washed and incubated with biotinylated goat-anti-hamster (Sigma-Aldrich, St. Louis, MO) Ab. All sections were again washed and incubated with Avidin/Biotinylated Enzyme Complex (ABC, Vector Laboratories Inc. Burlingame, CA). A final wash was performed before the addition of 3, 3-Diaminobenzidine (DAB) and counterstaining in Mayer's Hematoxylin. Cells staining positive for each specific Ab were counted in the 10 representative fields at × 400 magnification. The IF staining was performed as previously described (29), with modifications. Briefly, slides were rehydrated in PBS and 0.1% avidin blocking solution was applied to neutralize endogenous biotin. Sections were washed, blocked with 3% BSA in PBS containing 0.01% Triton X-100 (primary Ab diluent) and incubated overnight at 4°C with cell-specific antibodies in primary Ab diluent, along with anti-IpaB or anti-IpaD mAbs (generously provided by Dr. Edwin V. Oaks at the Department of Subunit Enteric Vaccines and Immunology, Bacterial Diseases Branch, Walter Reed Army Institute of Research, Silver Spring, MD). The following day, sections were washed with 0.1 % Triton X-100 followed by PBS. Biotin-conjugated goat anti-hamster Ab (Invitrogen) was used to detect anti-CD11c primary antibodies and goat anti-rat Ab (Invitrogen) was used to detect anti-rER-MP23, anti-Ly-6G (Gr-1) (clone: RB6-8C5) (AbD Serotec, Raleigh, NC), anti-CD-40 (clone: 3/23) (BD Biosciences) and CD207 Abs, both prepared in the primary diluent buffer. Alexa Flour 488 goat anti-mouse (Invitrogen) was added to detect the antigen-specific antibodies. The stained slides were again washed and incubated in streptavidin conjugated to Alexa Flour 568 (Invitrogen). After another wash, DAPI was added to all the slides to stain the nucleus and the slides were mounted using VECTASHIELD mounting media (Vector Laboratories, Burlingame, CA). IF staining was visualized using a Nikon A1 confocal laser microscope for acquisition of images and at least six 7 μm z-stack projections were collected at 0.300 – 0.400 μm intervals using the Nikon Elements Microscope Imaging Software (Nikon Instruments, Inc., Melville, NY). Manders overlap coefficient of the red channel (M_{red}) was calculated using the Volocity 3D Image Analysis Software (Improvision-Perkin-Elmer, Waltham, MA) to determine the extent of colocalization between cells that stained positively for a particular immune cell marker (detected with Alexa Flour 568 in the red channel) as well as the Ipas (Alexa Flour 488 under the green channel). The M_{red} represents the total sum of voxels of the overlapped red with green components divided by the total sum of red intensities. M_{red} was reported for each treatment as an average of the 4 to 6 z-stack images where the threshold was adjusted to 5% for all images to compensate for any background noise. The confocal image acquisition and analyses were adopted from published reports (30).

Statistical analysis

Statistical analyses were performed using GraphPad Prism 6 (GraphPad Software, Inc., La Jolla, CA). For IHC and IF, statistically significant differences for each cell type were determined by One-Way ANOVA with Bonferroni's and Tukey's multiple comparisons

tests, respectively, comparing tissue from vaccine versus PBS recipients. Two-Way ANOVA with Bonferroni's multiple comparisons test was used to determine statistical significance of the differences between serum Ab titers of vaccinated versus control groups. Significant differences between ASC, cytokine and stool IgA of vaccinated versus control mice were determined by One-Way ANOVA with Bonferroni's multiple comparisons test. Unpaired t-test with a 95% confidence interval was used to compare IgG1 and IgG2a subclass titers in vaccine versus PBS group. Mean Ab titers in mucosal fluids of vaccine recipients versus PBS were compared by One-Way ANOVA with Dunnett's multiple comparisons test. Survival curves were compared using a logrank (Mantel-Cox) test. In all analyses, differences were considered statistically significant if p values were ≤ 0.05.

Results

Inoculum distribution and recruitment of immune cells following i.d. vaccination

We investigated i.d. delivery of IpaB and IpD adjuvanted with the *E. coli* dmLT as a novel and potentially more efficient approach (than oral delivery) for immunization against shigellosis. The vaccine was administered to mice on 3 occasions, 2 wks apart, using NanoPass MicronJet 600 microneedles. To establish the optimal conditions for vaccination, we first performed a series of experiments using India ink to better visualize the inoculum distribution. An inoculum volume of 25 μl was identified as optimal as it produced a visible and consistent skin bleb without leakage (Supplemental Figure 1A). To confirm delivery into the dermis and to visualize changes in tissue morphology, the skin tissue was examined. During the first 4 h after infection, the dye was seen as a thick dark blue layer confined to the dermal space (Supplemental Figure 1B). At 24 h, the ink strip was tangential to the skin surface and large numbers of phagocytic cells (mostly neutrophils and some macrophages) had been recruited. One week after injection, the dye had diffused throughout the tissue and had been almost completely ingested by phagocytic cells (Supplemental Figure 1).

We next investigated the changes in cell composition following i.d. vaccination with IpaB, IpaD and dmLT. The presence of neutrophils, macrophages, DC, LC, $CD4^+$ and $CD8^+$ T cells in skin tissue was evaluated by H&E and IHC staining and confirmed by morphological analysis. Tissue from mice injected with PBS was included as control. Neutrophils rapidly infiltrated the injection site; the largest numbers were detected 4 h after injection and then gradually declined, remaining elevated for at least 1 wk (Figure 1A). Macrophages were also recruited, albeit at lower numbers and a more gradual pace, reaching their peak at the 1 wk time point (Figure 1A). $CD11c^+$ DC and $CD207^+$ ($Langerin^+$) LC were likewise detected; these cells significantly increased 24 h after vaccination and persisted elevated for at least 1 wk. At either time point, the recruited DC outnumbered the LC. Interestingly, $CD4^+$ and $CD8^+$ T cells were also recruited to the vaccination site after 24 h, with the highest numbers detected 1 wk post-injection (Figure 1C). Representative IHC images for each cell type in control and vaccinated mice at peak time points are shown on Figure 1A-C, right panels.

Vaccine uptake by innate immune cells

Next, we looked at the cells that might be involved in vaccine uptake by performing IF staining and confocal laser microscopy. For this analysis, we focused the z-stacks (images of planes at various depths) on tissue sections with abundant staining to investigate the presence of IpaB and IpaD (green) within specific cells, e.g., $CD11c^+$ cells (red). The images displayed in Figure 2A clearly show positive staining for IpaB and IpaD colocalized with $CD11c^+$ DC in tissue sections from vaccinated mice, as well as the absence of relevant staining in unvaccinated controls. To determine the extent of antigen sampling, we measured colocalization of IpaB and IpaD within $CD11c^+$ DC through calculation of M_{red} coefficient, whereby a value of 1.0 indicates the maximum colocalization of vaccine Ag within $CD11c^+$ cells and a value of ~0.1 represents baseline (mean value for IpaB and IpaD colocalization within $CD11c^+$ cells in the PBS controls). Skin DC containing IpaB or IpaD were detected as early as 4 h after vaccination; in fact, DC containing IpaB were still observed 1 wk post vaccination (Figure 2B). Based on these results and in the superior immunogenicity observed in parallel experiments (described below), we focused on IpaB in subsequent studies to investigate cells involved in antigen sampling as a pre-requisite for induction of adaptive immunity. We hypothesized that IpaB would be likewise taken up by other immune cells in the skin, particularly LC, which are extremely efficient APC. IpaB was found within neutrophils ($Ly\text{-}6G^+$) 24 h and 1 wk post vaccination. IpaB staining also colocalized with LC and skin macrophages ($ER\text{-}MP23^+$) at all time points examined (Figure 3). The fluorescence intensity of IpaB overlapping that of DC, LC and macrophages was not significantly different, suggesting a similar vaccine sampling capacity for these cell types, with colocalized Ag staining seen as early as 4 h and up to 1 wk after vaccination. We also investigated the activated phenotype ($CD40^+$) of IpaB-containing APC and found significant overlap between IpaB and $CD40^+$ cell fluorescent staining 24 h and 1 wk after vaccination.

Serum Ab responses induced by i.d. delivered IpaB, IpaD and dmLT

We first conducted a dose-escalation experiment in which low, medium and high dosage levels of IpaB and IpaD, alongside a constant amount of the *E. coli* dmLT, were administered i.d. to BALB/c mice (Figure 4A). Groups immunized with the same Ag i.n. served as positive controls, while negative controls received dmLT and PBS. Intradermal immunization with IpaB and IpaD resulted in high levels of antigen-specific serum IgG antibodies, regardless of the dose administered. Peak serum IgG responses to IpaB were achieved after the second vaccination and the magnitude appeared to be similar for all groups (Figure 4B). The IpaB IgG responses produced by i.d. immunization were somewhat lower, however, than the responses induced by the protein administered i.n. For IpaD, all groups reached similar (peak) IgG levels at the time of challenge. In contrast to IpaB, however, the dosage level did influence the kinetics of IgG production. The high dose group exhibited a faster Ab response to IpaD, attaining peak levels after the second vaccination, whereas the low dose group required an additional immunization to reach the same level of response. It was also noticed that the IgG titers against IpaD produced by i.d. vaccination were lower than those produced by i.n. immunization. Very high IgG responses to dmLT were also elicited by the i.d. vaccinated mice, which were very similar among groups, proving the consistency of the procedures.

Interestingly, we failed to detect antigen-specific IgA for any of the proteins (IpaB, IpaD or dmLT) in stool supernatants following i.d. vaccination. No IgA could be detected in serum either (data not shown). We did, however, detect positive fecal IgA responses against all three Ag in mice immunized i.n. (Figure 4C). No Ab responses were detected in the unvaccinated (PBS) controls.

ASC induced by i.d. immunization with IpaB, IpaD and dmLT

To further investigate the induction of mucosal immune responses, we measured IpaB, IpaD and dmLT-specific IgG and IgA ASC in the lungs at the time of challenge. No responses were detected in mice vaccinated i.d. whereas significant numbers of IgG and IgA ASC were seen in mice immunized i.n. (Figure 5). We also measured the frequency of IpaB-, IpaD- and dmLT-specific ASC in spleen and bone marrow (Figure 5). Mice immunized i.d. exhibited IgG ASC responses to IpaB and IpaD in both organs, which, for the most part, increased with the vaccine dose (Figure 5). IgG ASC specific for dmLT were also produced following i.d. vaccination. To our surprise, only IgG (not IgA) ASC were elicited in response to i.d. immunization; the same was observed for all three vaccine Ag, irrespective of the vaccine dose administered. On the other hand, i.n. vaccination induced both IgG and IgA antigen-specific ASC in all tissues examined. The IgG ASC responses measured in the spleen and bone marrow of the medium and high dose i.d. groups were comparable to those induced by i.n. vaccination. No responses were detected in the unvaccinated control.

Production of cytokines upon in vitro antigen stimulation

We next examined the production of Th1, Th2, pro-inflammatory and regulatory cytokines by spleen cells stimulated in vitro with IpaB or IpaD. All groups immunized i.d showed increased production of IL-2, as well as IFN-γ and TNF-α in response to IpaB (Figure 6). These same cytokines, and similar magnitude of responses, were detected after i.n. vaccination (Figure 6). IL-17 was also produced by mice immunized i.d. in response to IpaB, particularly the high and medium dose groups (Figure 6). IL-2 was the only Th1 type cytokine produced at significant levels in response to IpaD by i.d. vaccinated mice. Very high levels of Th2-type cytokines (IL-4 and IL-5) were produced by spleen lymphocytes in response to both IpaB and IpaD following i.d. vaccination (Figure 6). The secretion of IL-4 and IL-5 by cells stimulated with IpaB was noteworthy as it greatly exceeded that of mice immunized i.n. The same was observed for IL-5 against IpaD. IL-10 was also produced by i.d. vaccinated mice in response to IpaB and IpaD (Figure 6, top panel).

Antigen-specific induction of IFN-γ, IL-2 and IL-5 was increased in the inguinal and popliteal DLN as a result of i.d. vaccination. These responses were remarkably high in the group that received the medium dose of vaccine and in response to IpaB (Figure 6, bottom panel). As expected, negligible responses were seen in mice immunized i.n. No responses were detected in the dmLT and PBS controls.

Protection against lethal S. flexneri pulmonary challenge

Intradermal vaccination with IpaB, IpaD and dmLT afforded significant protection against lethal pulmonary infection with *S. flexneri*. The group that received the medium dosage level had the highest survival rate (70%). Significant protection was also observed in the group

that received the lowest dose (20%). Unexpectedly, all of the mice immunized with the highest dose of IpaB and IpaD succumbed to challenge (Figure 7). The difference in protection between the medium and high dose groups prompted us to perform a second experiment to confirm these findings.

Immune responses to IpaB and IpaD with or without E. coli dmLT

A second experiment was performed to: 1) ascertain the superior protection of the intermediate dosage level, 2) investigate cross-protection against a different *Shigella* serotype (*S. sonnei*); and to 3) assess the adjuvant contribution of dmLT in the responses induced. Mice were immunized with the high and medium dosage level of IpaB and IpaD as described above and the proteins were given alone or in the presence of dmLT. A positive control group received IpaB, IpaD and dmLT i.n. and a negative control group received PBS (Figure 8A). The IpaB protein used in this experiment had the IpgC chaperone removed. Similar to what was observed in the first experiment, high levels of IpaB and IpaD serum IgG were produced by the proteins given i.d. admixed with dmLT. The medium dose group produced higher IgG responses against IpaB and interestingly, these titers (as well as those measured in the high dose group) surpassed those seen in the first experiment, suggesting a higher immunogenic capacity of IpaB compared to IpaB/IpgC when administered via the i.d. route. No differences were seen in the IpaD responses between dosage groups or experiments. The dmLT significantly enhanced the serum IgG responses to both IpaB and IpaD, as compared to the proteins given alone (Figure 8B). Serum IgG responses to dmLT were also elicited, which were similar among the i.d vaccinated groups across experiments. A side-by-side comparison of the Ab responses obtained in both experiments is shown in Supplemental Table 1.

Serum IgG2a/IgG1 subclasses and mucosal IgG and IgA antibodies

In this experiment, we also examined the IgG subclass profile induced by i.d. vaccination with IpaB and IpaD with or without dmLT. High levels of IgG1 were produced in response to IpaB and IpaD, which were similar for the medium and high dosage levels (Figure 9A). IgG2a was also produced, albeit at lower levels and similarly unaffected by the dose. The presence of dmLT allowed for increased production of IgG2a. IgG1 and IgG2a were produced in response to dmLT and levels were similar in all dmLT recipients.

We also investigated the presence of IgG and IgA antibodies in the mucosal airways. IpaB- and IpaD-specific IgG were detected in BALF of mice immunized with the Ipas admixed with dmLT. The titers were significantly lower in the absence of dmLT, and this was particularly noticeable in the responses to IpaD (Figure 9B). IgG antibodies against dmLT were also detected; titers were similar for both i.d. groups and comparable to those measured in the i.n. control group. We were unable to detect vaccine-specific IgA in the alveolar fluid of the i.d. vaccinated mice. In contrast, IgA specific for all 3 vaccine Ag were present by in the BALF of mice immunized i.n. The amounts of total IgG and IgA among individual samples were not significantly different, thus confirming homogenous sampling (data not shown). It was noticed, however, that the fluids of mice immunized i.n. contained larger quantities of total antibodies than immunized i.d. (data not shown); this was deemed consistent with nasal exposure activating (local) mucosal immunity.

Protection against S. flexneri and S. sonnei lethal pulmonary challenge

In agreement with our previous results, 70% of the mice that received the medium dose of IpaB and IpaD admixed with dmLT survived the challenge with virulent *S. flexneri* (Figure 10A). In the absence of dmLT, the protection dropped to 50%. In contrast, the groups immunized with the highest dose of IpaB and IpaD, had 30-40% protection with the dmLT providing no apparent improvement (Figure 10A). Immunization with the medium dose of IpaB and IpaD plus dmLT also resulted in significant (50%) protection against *S. sonnei* (Figure 10B). The percent survival dropped to 20% in the absence of dmLT. In both challenges, 100% protection was seen in the positive control group (Figure 10).

Discussion

The recent Global Enteric Multicenter Study identified *Shigella* as a top priority intervention target to reduce illness and death caused by diarrheal disease in children under the age of five years of age in low-income countries (1). We have proposed the use of *Shigella* TTSS proteins IpaB and IpaD as protective Ag to formulate a broadly protective *Shigella* vaccine. The need for practical and effective ways to deliver such a vaccine prompted us to investigate the i.d. route of immunization which, coupled with new technologies, has emerged as suitable alternative to intramuscular injection as it is similarly effective and yet more practical and less painful. The fact that it has been the route of immunization for eradication of smallpox and continues to be successfully used to administer BCG to millions of children around the world provides a formidable precedent for its use to prevent enteric diseases in resource-poor areas. We demonstrated in this study that i.d. delivery of *Shigella* IpaB and IpaD admixed with the *E. coli* dmLT is a simple and effective approach to induce protective immunity against lethal infection caused by different *Shigella* serotypes. To our knowledge, this is the first report of successful i.d. immunization with a cross-protective, subunit-based *Shigella* vaccine.

Multiple devices have been developed to facilitate i.d. vaccine delivery that are easy to use and more reliable than the conventional needle and syringe techniques (19). The NanoPass hollow microneedles used in this study allow delivery of the inoculum (even highly viscuous substances) into the dermis in a slow and controlled manner. This device has been approved by the FDA and was safe, effective and reliable in clinical studies of i.d. influenza vaccination (31,32). The microneedles are barely noticeable (shorter than 1 mm) and slightly penetrate the skin, thus greatly reducing pain (and the perception of pain). Different from traditional i.d. injection with needle and syringe (i.e., Mantoux technique), which requires highly trained personnel, i.d. injection with microneedles is easier and vaccines could potentially be self-administered at home (19,33). To our knowledge, this is the first report of a preclinical vaccine study using the NanoPass microneedles.

Our results demonstrate consistent delivery of vaccine into the dermis and the ensuing activation of an innate immune response with immediate recruitment of large numbers of neutrophils, followed by macrophages, DC and LC. Our finding of $CD11c^+$ DC, LC and macrophages containing IpaB, and the evidence of cell activation, imply that these cells participate in Ag sampling and shuttling to the DLN for T cell stimulation (34). In fact, the success of i.d. vaccination is predicated on the efficiency of this process. The presence of

IpaB- and IpaD-specific cytokine-secreting T cells in the inguinal lymph nodes of i.d. vaccinated mice supports this notion. In addition, the recruitment of $CD4^+$ and $CD8^+$ T cells and activated antigen-carrying APC in the dermis up to 1 wk after vaccination suggests the possibility of local T cell priming. The presence of $CD8^+$T cells is consistent with reports describing the involvement of skin-activated LC preferentially priming antigen-specific $CD8^+$ T cells after i.d. vaccination (34,35).

Intradermal immunization with IpaB, IpaD and dmLT resulted in high levels of antigen-specific serum IgG and systemic (spleen and bone marrow) IgG ASC. A distinct, unanticipated observation was the lack of serum IgA, systemic IgA ASC, and mucosal (stool and BALF) IgA when the Ag were administered i.d. Similarly unexpected was the absence of ASC in the lungs (IgG or IgA) at the time of challenge - presumably needed to secrete mucosal antibodies to clear the pathogen, and yet these animals were largely protected. Considering that the timing of ASC sampling might not have been optimal (since mucosal responses usually peak soon after vaccination), we measured lung ASC and Abs in the airways 1 wk after the last immunization. While the ASC results were mostly negative (data not shown), high levels of IgG were found in the BALF of i.d. vaccinated mice. Still, no IgA was found. In the absence of lung ASC, it could be argued that the IgG detected in the BALF possibly derive from ASC residing in other parts of the respiratory tract or from systemic sources, i.e., circulating or spleen plasmablasts and plasma cells. These antibodies may reach the mucosa by transudation or through active transport via the FcRn (36). The extent to which systemic immunity contributes to protection against *Shigella* is unclear. In humans, serum IgG antibodies to LPS have been associated with serotype-specific protection [Reviewed in (6)]. It has been hypothesized that these antibodies transudate into the gut where they may neutralize and/or kill the organism, possibly through complement activation (37,38). Serum IgG against IpaB was correlated with reduced disease severity in challenged individuals (14). Because the Ipas are expressed briefly upon bacterial-host cell contact, these antibodies presumably block invasion by preventing translocation of virulent factors. Others have proposed that if the mucosal defenses fail, the inflammatory process that accompanies *Shigella* infection may also lead to transudation of serum IgG into the lamina propria and thereby limit tissue invasion (39).

Precedent exists for routine parenteral vaccines that preferentially induce systemic immunity to prevent mucosal infections (e.g., pneumococcal and *Haemophilus influenzae* type b conjugates, *Salmonella* Typhi Vi and pertussis vaccines). The same principle may operate in our model of i.d. immunization with IpaB and IpaD and lung exposure to virulent *Shigella*. Meanwhile, robust mucosal and systemic IgG and IgA ASC and antibodies directed to all vaccine Ag were seen in mice immunized i.n. These differences likely reflect distinct pathways of immunological priming, with i.d. immunization favoring the induction of systemic IgG and i.n. immunization both systemic and mucosal IgA and IgG. The high (and seemingly exclusive) IgG levels produced by i.d. vaccination could be explained, in part, by the fact that Ag delivered i.d. have access to dermal DC, which induce differentiation of naïve T cells into T follicular helper cells, a subset that contributes to class switch and proliferation of B cells within germinal centers (34). Strikingly high levels of IL-4 and IL-5 were produced by antigen-stimulated T cells from i.d. vaccinated mice. Skin LC are known

to induce $CD4^+$Th2 cell differentiation (40). Thus, the demonstration of $CD207^+$ DC carrying vaccine Ag in our study is consistent with the unusually high levels of Th2 type cytokines observed, which largely surpassed those of the i.n. group. Vaccine-induced T cells also produced IL-2 and IFN-γ as well as IL-10, indicating that Th1-type and T regulatory responses were likewise induced.

IpaB was the most immunogenic of the two proteins (both for antibodies and T cell responses) in agreement with results from previous studies (15,16). The dmLT adjuvant increased Ab production and particularly the level of IgG2a, promoting a Th1-type response. This is the first preclinical demonstration of tolerability and robust adjuvanticity of the *E. coli* dmLT when administered i.d. alongside a protein subunit vaccine. A Phase 1 clinical study to evaluate the safety and immunogenicity of dmLT administered i.d. to humans is being planned by the Division of Microbiology and Infectious Diseases (DMID), at the National Institute of Allergy and Infectious Disease (NIAD) of the NIH, in collaboration with PATH.

Importantly, mice immunized i.d. with IpaB, IpaD and dmLT were protected from *S. flexneri* and *S. sonnei* lethal infection. The medium vaccine dosage was consistently the most effective. The larger death rate in the high dose group was unexpected, yet reproduced in two separate experiments. Interestingly, comparable levels of serum antibodies were elicited by the different dose groups, despite their distinct protective efficacy. The amount of circulating IgG against IpaB and IpaD, alone, does not correlate with protection in this model (16), which suggests that other immunological effectors contribute to protective immunity. However, antibodies are believed to play an important role in this process by blocking invasion and clearing the pathogen. In fact, early studies reported lack of protection in B cell deficient mice pre-exposed to sublethal doses of *Shigella* (as opposed to wild type) and prolonged survival of naïve mice upon passive transfer of immune sera (41). It is possible that the different vaccine doses might have induced antibodies of different quality and functional capacity that influenced the protective outcomes. A noticeable difference between the medium and high dose groups, which could help explain the dissimilar protection, was the increase in antigen-specific T cell cytokine responses (IFN-γ, IL-5, IL-2) in the DLN of the former. In a previous study, we found a correlation between IL-2, IL-5, IL-10 and IL-17 production and protection against lung infection in mice (16). IFN-γ, along with TNF-α, are believed to facilitate microbial clearance through recruitment and activation of phagocytic cells (42-44). The synthesis of IL-5, which stimulates B cell proliferation and antibody secretion, is consistent with supporting the vigorous IgG responses elicited by i.d vaccination whereas IL-2, which induces proliferation and differentiation of T and B cells, is expected to centrally regulate the responses induced. IL-17, which was detected in culture supernatants from Ag-stimulated spleen cells of i.d. vaccinated mice, has been shown to restrict bacterial growth in infected murine lungs (45). IL-10, also produced by spleen cells, may play a role in controlling inflammation and modulating T and B cell responses. T cells primed by skin-derived APC in regional lymph nodes are presumably endowed with the capacity to migrate to distant effector sites where they can help circumscribe the infection. It is possible that an excess of antigen in the high dose group may have compromised the processes of antigen uptake and/or presentation to T

cells. Another potential reason for the superior T cell responses and protection of the medium dosage group is the higher adjuvant:antigen ratio these animals received. While the amount of IpaB and IpD in the vaccines for the different groups increased, the dmLT remained constant, and this amount might have been insufficient or masked as more Ag was added. Thus it could be assumed that optimal adjuvanticity was seemingly achieved for the medium dose treatment. These results emphasize the need to test different antigen-adjuvant combinations in future vaccine studies to draw valid conclusions.

While the vaccine-sparing advantage of i.d. over parenteral vaccination has been reported, little is known on how i.d. compares with mucosal immunization. Beyond the differences in the type and magnitude of immune responses induced, both the i.n. and the i.d. routes of immunization conferred significant levels of protection, with i.d. vaccination requiring 25-40 times smaller dose. The use of the same route for immunization and challenge provides an “immunological advantage” that may account for the higher protection conferred by i.n. vaccination. Although successful in mice, an IpaB/IpaD dmLT vaccine could not be administered via the nasal route to humans because of safety concerns associated with the use of an enterotoxin-derived adjuvant (46,47). It has also been argued that i.n vaccination of children living in poor resource (endemic) areas might be difficult due to their frequent respiratory infections and symptomatic runny noses, which may interfere with vaccine take (48). An i.d. IpaB and IpaD *Shigella* vaccine would be preferable, as it is expected to be safer, potentially more effective (not blocked by mucosal barriers), and applicable to large-scale immunization based on the precedent of BCG.

In conclusion, to our knowledge, our results provide the first preclinical evidence of cross-protective immunity of i.d. delivered IpaB and IpaD against *Shigella* infection. The efficiency, ease of delivery, improved safety (avoiding the use of needles), and reduced cost (due to dose-sparing) of i.d. vaccination are appealing features for implementing this approach to immunize against shigellosis children who live in high-risk areas, using an IpaB and IpaD-broad spectrum vaccine. These results and considerations warrant further investigation of i.d. delivered IpaB and IpaD in humans.

Supplementary Material

Refer to Web version on PubMed Central for supplementary material.

Acknowledgments

We thank Elizabeth Smith (Center for Vascular and Inflammatory Diseases Histology Core Facility, University of Maryland School of Medicine) and Joseph A. Roche (Department of Physiology, University of Maryland School of Medicine) for their assistance with histology and immunolabeling procedures. The authors acknowledge Dr. Yotam Levine (NanoPass Technologies) for providing the MicronJet needles and technical expertise, Dr. Ed Oaks (WRAIR) for kindly providing the IpaB and IpaD monoclonal antibodies and Amanda Buskirk (CVD) for critical review of the manuscript. We also thank members of the CVD Applied Immunology Section and the Picking laboratory for technical support.

This research was funded by PATH and in part by NIH R01 AI089519 (to MFP and WLP).

References

1. Kotloff KL, Nataro JP, Blackwelder WC, Nasrin D, Farag TH, Panchalingam S, Wu Y, Sow SO, Sur D, Breiman RF, Faruque AS, Zaidi AK, Saha D, Alonso PL, Tamboura B, Sanogo D, Onwuchekwa U, Manna B, Ramamurthy T, Kanungo S, Ochieng JB, Omore R, Oundo JO, Hossain A, Das SK, Ahmed S, Qureshi S, Quadri F, Adegbola RA, Antonio M, Hossain MJ, Akinsola A, Mandomando I, Nhampossa T, Acacio S, Biswas K, O'Reilly CE, Mintz ED, Berkeley LY, Muhsen K, Sommerfelt H, Robins-Browne RM, Levine MM. Burden and aetiology of diarrhoeal disease in infants and young children in developing countries (the Global Enteric Multicenter Study, GEMS): a prospective, case-control study. Lancet. 2013; 382:209–222. [PubMed: 23680352]
2. Lozano R, Naghavi M, Foreman K, Lim S, Shibuya K, Aboyans V, Abraham J, Adair T, Aggarwal R, Ahn SY, Alvarado M, Anderson HR, Anderson LM, Andrews KG, Atkinson C, Baddour LM, Barker-Collo S, Bartels DH, Bell ML, Benjamin EJ, Bennett D, Bhalla K, Bikbov B, Bin AA, Birbeck G, Blyth F, Bolliger I, Boufous S, Bucello C, Burch M, Burney P, Carapetis J, Chen H, Chou D, Chugh SS, Coffeng LE, Colan SD, Colquhoun S, Colson KE, Condon J, Connor MD, Cooper LT, Corriere M, Cortinovis M, de Vaccaro KC, Couser W, Cowie BC, Criqui MH, Cross M, Dabhadkar KC, Dahodwala N, De LD, Degenhardt L, Delossantos A, Denenberg J, Des Jarlais DC, Dharmaratne SD, Dorsey ER, Driscoll T, Duber H, Ebel B, Erwin PJ, Espindola P, Ezzati M, Feigin V, Flaxman AD, Forouzanfar MH, Fowkes FG, Franklin R, Fransen M, Freeman MK, Gabriel SE, Gakidou E, Gaspari F, Gillum RF, Gonzalez-Medina D, Halasa YA, Haring D, Harrison JE, Havmoeller R, Hay RJ, Hoen B, Hotez PJ, Hoy D, Jacobsen KH, James SL, Jasrasaria R, Jayaraman S, Johns N, Karthikeyan G, Kassebaum N, Keren A, Khoo JP, Knowlton LM, Kobusingye O, Koranteng A, Krishnamurthi R, Lipnick M, Lipshultz SE, Ohno SL, Mabweijano J, MacIntyre MF, Mallinger L, March L, Marks GB, Marks R, Matsumori A, Matzopoulos R, Mayosi BM, McAnulty JH, McDermott MM, McGrath J, Mensah GA, Merriman TR, Michaud C, Miller M, Miller TR, Mock C, Mocumbi AO, Mokdad AA, Moran A, Mulholland K, Nair MN, Naldi L, Narayan KM, Nasseri K, Norman P, O'Donnell M, Omer SB, Ortblad K, Osborne R, Ozgediz D, Pahari B, Pandian JD, Rivero AP, Padilla RP, Perez-Ruiz F, Perico N, Phillips D, Pierce K, Pope CA III, Porrini E, Pourmalek F, Raju M, Ranganathan D, Rehm JT, Rein DB, Remuzzi G, Rivara FP, Roberts T, De Leon FR, Rosenfeld LC, Rushton L, Sacco RL, Salomon JA, Sampson U, Sanman E, Schwebel DC, Segui-Gomez M, Shepard DS, Singh D, Singleton J, Sliwa K, Smith E, Steer A, Taylor JA, Thomas B, Tleyjeh IM, Towbin JA, Truelsen T, Undurraga EA, Venketasubramanian N, Vijayakumar L, Vos T, Wagner GR, Wang M, Wang W, Watt K, Weinstock MA, Weintraub R, Wilkinson JD, Woolf AD, Wulf S, Yeh PH, Yip P, Zabetian A, Zheng ZJ, Lopez AD, Murray CJ. Global and regional mortality from 235 causes of death for 20 age groups in 1990 and 2010: a systematic analysis for the Global Burden of Disease Study 2010. Lancet. 2012; 380:2095–2128. [PubMed: 23245604]
3. Murray CJ, Vos T, Lozano R, Naghavi M, Flaxman AD, Michaud C, Ezzati M, Shibuya K, Salomon JA, Abdalla S, Aboyans V, Abraham J, Ackerman I, Aggarwal R, Ahn SY, Ali MK, Alvarado M, Anderson HR, Anderson LM, Andrews KG, Atkinson C, Baddour LM, Bahalim AN, Barker-Collo S, Barrero LH, Bartels DH, Basanez MG, Baxter A, Bell ML, Benjamin EJ, Bennett D, Bernabe E, Bhalla K, Bhandari B, Bikbov B, Bin AA, Birbeck G, Black JA, Blencowe H, Blore JD, Blyth F, Bolliger I, Bonaventure A, Boufous S, Bourne R, Boussinesq M, Braithwaite T, Brayne C, Bridgett L, Brooker S, Brooks P, Brugha TS, Bryan-Hancock C, Bucello C, Buchbinder R, Buckle G, Budke CM, Burch M, Burney P, Burstein R, Calabria B, Campbell B, Canter CE, Carabin H, Carapetis J, Carmona L, Cella C, Charlson F, Chen H, Cheng AT, Chou D, Chugh SS, Coffeng LE, Colan SD, Colquhoun S, Colson KE, Condon J, Connor MD, Cooper LT, Corriere M, Cortinovis M, de Vaccaro KC, Couser W, Cowie BC, Criqui MH, Cross M, Dabhadkar KC, Dahiya M, Dahodwala N, Damsere-Derry J, Danaei G, Davis A, De LD, Degenhardt L, Dellavalle R, Delossantos A, Denenberg J, Derrett S, Des Jarlais DC, Dharmaratne SD, Dherani M, Diaz-Torne C, Dolk H, Dorsey ER, Driscoll T, Duber H, Ebel B, Edmond K, Elbaz A, Ali SE, Erskine H, Erwin PJ, Espindola P, Ewoigbokhan SE, Farzadfar F, Feigin V, Felson DT, Ferrari A, Ferri CP, Fevre EM, Finucane MM, Flaxman S, Flood L, Foreman K, Forouzanfar MH, Fowkes FG, Fransen M, Freeman MK, Gabbe BJ, Gabriel SE, Gakidou E, Ganatra HA, Garcia B, Gaspari F, Gillum RF, Gmel G, Gonzalez-Medina D, Gosselin R, Grainger R, Grant B, Groeger J, Guillemin F, Gunnell D, Gupta R, Haagsma J, Hagan H, Halasa YA, Hall W, Haring D, Haro JM, Harrison JE, Havmoeller R, Hay RJ, Higashi H, Hill C, Hoen B, Hoffman H, Hotez PJ, Hoy D, Huang JJ, Ibeanusi SE,

Jacobsen KH, James SL, Jarvis D, Jasrasaria R, Jayaraman S, Johns N, Jonas JB, Karthikeyan G, Kassebaum N, Kawakami N, Keren A, Khoo JP, King CH, Knowlton LM, Kobusingye O, Koranteng A, Krishnamurthi R, Laden F, Lalloo R, Laslett LL, Lathlean T, Leasher JL, Lee YY, Leigh J, Levinson D, Lim SS, Limb E, Lin JK, Lipnick M, Lipshultz SE, Liu W, Loane M, Ohno SL, Lyons R, Mabweijano J, MacIntyre MF, Malekzadeh R, Mallinger L, Manivannan S, Marcenes W, March L, Margolis DJ, Marks GB, Marks R, Matsumori A, Matzopoulos R, Mayosi BM, McAnulty JH, McDermott MM, McGill N, McGrath J, Medina-Mora ME, Meltzer M, Mensah GA, Merriman TR, Meyer AC, Miglioli V, Miller M, Miller TR, Mitchell PB, Mock C, Mocumbi AO, Moffitt TE, Mokdad AA, Monasta L, Montico M, Moradi-Lakeh M, Moran A, Morawska L, Mori R, Murdoch ME, Mwaniki MK, Naidoo K, Nair MN, Naldi L, Narayan KM, Nelson PK, Nelson RG, Nevitt MC, Newton CR, Nolte S, Norman P, Norman R, O'Donnell M, O'Hanlon S, Olives C, Omer SB, Ortblad K, Osborne R, Ozgediz D, Page A, Pahari B, Pandian JD, Rivero AP. Disability-adjusted life years (DALYs) for 291 diseases and injuries in 21 regions, 1990-2010: a systematic analysis for the Global Burden of Disease Study 2010. Lancet. 2012; 380:2197–2223. [PubMed: 23245608]

4. Levine MM. Enteric infections and the vaccines to counter them: future directions. Vaccine. 2006; 24:3865–3873. [PubMed: 16603279]
5. Barry EM, Pasetti MF, Sztein MB, Fasano A, Kotloff KL, Levine MM. Progress and pitfalls in Shigella vaccine research. Nat Rev Gastroenterol Hepatol. 2013; 10:245–255. [PubMed: 23419287]
6. Levine MM, Kotloff KL, Barry EM, Pasetti MF, Sztein MB. Clinical trials of *Shigella* vaccines: two steps forward and one step back on a long, hard road. Nat Rev Microbiol. 2007; 5:540–553. [PubMed: 17558427]
7. Venkatesan MM, Ranallo RT. Live-attenuated Shigella vaccines. Expert Rev Vaccines. 2006; 5:669–686. [PubMed: 17181440]
8. Kaminski RW, Oaks EV. Inactivated and subunit vaccines to prevent shigellosis. Expert Rev Vaccines. 2009; 8:1693–1704. [PubMed: 19943764]
9. Picking WL, Nishioka H, Hearn PD, Baxter MA, Harrington AT, Blocker A, Picking WD. IpaD of Shigella flexneri is independently required for regulation of Ipa protein secretion and efficient insertion of IpaB and IpaC into host membranes. Infect Immun. 2005; 73:1432–1440. [PubMed: 15731041]
10. Marteyn B, Gazi A, Sansonetti P. Shigella: a model of virulence regulation in vivo. Gut Microbes. 2012; 3:104–120. [PubMed: 22356862]
11. Robin G, Cohen D, Orr N, Markus I, Slepon R, Ashkenazi S, Keisari Y. Characterization and quantitative analysis of serum IgG class and subclass response to Shigella sonnei and Shigella flexneri 2a lipopolysaccharide following natural Shigella infection [In Process Citation] Characterization and quantitative analysis of serum IgG class and subclass response to Shigella sonnei and Shigella flexneri 2a lipopolysaccharide following natural Shigella infection. J Infect Dis. 1997; 175:1128–1133. [PubMed: 9129076]
12. Oberhelman RA, Kopecko DJ, Salazar-Lindo E, Gotuzzo E, Buysse JM, Venkatesan MM, Yi A, Fernandez-Prada C, Guzman M, Leon-Barua R. Prospective study of systemic and mucosal immune responses in dysenteric patients to specific Shigella invasion plasmid antigens and lipopolysaccharides. Infect Immun. 1991; 59:2341–2350. [PubMed: 2050402]
13. Van de Verg LL, Herrington DA, Boslego J, Lindberg AA, Levine MM. Age-specific prevalence of serum antibodies to the invasion plasmid and lipopolysaccharide antigens of Shigella species in Chilean and North American populations. J Infect Dis. 1992; 166:158–161. [PubMed: 1607690]
14. Wahid R, Simon JK, Picking WL, Kotloff KL, Levine MM, Sztein MB. Shigella antigen-specific B memory cells are associated with decreased disease severity in subjects challenged with wild-type Shigella flexneri 2a. Clin Immunol. 2013; 148:35–43. [PubMed: 23649043]
15. Martinez-Becerra FJ, Kissmann JM, Diaz-McNair J, Choudhari SP, Quick AM, Mellado-Sanchez G, Clements JD, Pasetti MF, Picking WL. Broadly protective Shigella vaccine based on type III secretion apparatus proteins. Infect Immun. 2012; 80:1222–1231. [PubMed: 22202122]
16. Heine SJ, Diaz-McNair J, Martinez-Becerra FJ, Choudhari SP, Clements JD, Picking WL, Pasetti MF. Evaluation of immunogenicity and protective efficacy of orally delivered Shigella type III secretion system proteins IpaB and IpaD. Vaccine. 2013; 31:2919–2929. [PubMed: 23644075]

17. Qadri F, Bhuiyan TR, Sack DA, Svennerholm AM. Immune responses and protection in children in developing countries induced by oral vaccines. Vaccine. 2012; 31:452–60. [PubMed: 23153448]
18. Pasetti MF, Simon JK, Sztein MB, Levine MM. Immunology of gut mucosal vaccines. Immunol Rev. 2011; 239:125–148. [PubMed: 21198669]
19. Kim YC, Jarrahian C, Zehrung D, Mitragotri S, Prausnitz MR. Delivery systems for intradermal vaccination. Curr Top Microbiol Immunol. 2012; 351:77–112. [PubMed: 21472533]
20. PATH. Intradermal delivery of vaccines: a review of the literature and the potential for development for use in low- and middle-income countries. 2013
21. Nelson KS, Janssen JM, Troy SB, Maldonado Y. Intradermal fractional dose inactivated polio vaccine: a review of the literature. Vaccine. 2012; 30:121–125. [PubMed: 22100886]
22. Sanofi Pasteur. [Accessed: September 10, 2013] Intanza®/ID Flu®, first intradermal influenza vaccine, approved in the European Union [Press Release]. 2009. Available at: http://www.sanofipasteur.com/sanofi-pasteur4/ImageServlet?imageCode=25356&siteCode=SP_CORP4.
23. Centers for Disease Control and Prevention. [Accessed: September 10, 2013] Intradermal influenza (flu) vaccination [Questions & answers]. 2013. Available at: http://www.cdc.gov/flu/protect/vaccine/qa_intradermal-vaccine.htm.
24. Hickling JK, Jones KR, Friede M, Zehrung D, Chen D, Kristensen D. Intradermal delivery of vaccines: potential benefits and current challenges. Bull World Health Organ. 2011; 89:221–226. [PubMed: 21379418]
25. Kupper TS, Fuhlbrigge RC. Immune surveillance in the skin: mechanisms and clinical consequences. Nat Rev Immunol. 2004; 4:211–222. [PubMed: 15039758]
26. Summerton NA, Welch RW, Bondoc L, Yang HH, Pleune B, Ramachandran N, Harris AM, Bland D, Jackson WJ, Park S, Clements JD, Nabors GS. Toward the development of a stable, freeze-dried formulation of *Helicobacter pylori* killed whole cell vaccine adjuvanted with a novel mutant of *Escherichia coli* heat-labile toxin. Vaccine. 2010; 28:1404–1411. [PubMed: 19897067]
27. Espina M, Olive AJ, Kenjale R, Moore DS, Ausar SF, Kaminski RW, Oaks EV, Middaugh CR, Picking WD, Picking WL. IpaD localizes to the tip of the type III secretion system needle of Shigella flexneri. Infect Immun. 2006; 74:4391–4400. [PubMed: 16861624]
28. Mach H, Middaugh CR, Lewis RV. Statistical determination of the average values of the extinction coefficients of tryptophan and tyrosine in native proteins. Anal Biochem. 1992; 200:74–80. [PubMed: 1595904]
29. Roche JA, Ford-Speelman DL, Ru LW, Densmore AL, Roche R, Reed PW, Bloch RJ. Physiological and histological changes in skeletal muscle following in vivo gene transfer by electroporation. Am J Physiol Cell Physiol. 2011; 301:C1239–C1250. [PubMed: 21832248]
30. Goldberg DS, Ghandehari H, Swaan PW. Cellular entry of G3.5 poly (amido amine) dendrimers by clathrin- and dynamin-dependent endocytosis promotes tight junctional opening in intestinal epithelia. Pharm Res. 2010; 27:1547–1557. [PubMed: 20411406]
31. Van DP, Oosterhuis-Kafeja F, Van der Wielen M, Almagor Y, Sharon O, Levin Y. Safety and efficacy of a novel microneedle device for dose sparing intradermal influenza vaccination in healthy adults. Vaccine. 2009; 27:454–459. [PubMed: 19022318]
32. Hung IF, Levin Y, To KK, Chan KH, Zhang AJ, Li P, Li C, Xu T, Wong TY, Yuen KY. Dose sparing intradermal trivalent influenza (2010/2011) vaccination overcomes reduced immunogenicity of the 2009 H1N1 strain. Vaccine. 2012; 30:6427–6435. [PubMed: 22910287]
33. Coleman BL, McGeer AJ, Halperin SA, Langley JM, Shamout Y, Taddio A, Shah V, McNeil SA. A randomized control trial comparing immunogenicity, safety, and preference for self- versus nurse-administered intradermal influenza vaccine. Vaccine. 2012; 30:6287–6293. [PubMed: 22902784]
34. Palucka K, Banchereau J, Mellman I. Designing vaccines based on biology of human dendritic cell subsets. Immunity. 2010; 33:464–478. [PubMed: 21029958]
35. Liard C, Munier S, Joulin-Giet A, Bonduelle O, Hadam S, Duffy D, Vogt A, Verrier B, Combadiere B. Intradermal immunization triggers epidermal Langerhans cell mobilization required for CD8 T-cell immune responses. J Invest Dermatol. 2012; 132:615–625. [PubMed: 22170490]

36. Rath T, Kuo TT, Baker K, Qiao SW, Kobayashi K, Yoshida M, Roopenian D, Fiebiger E, Lencer WI, Blumberg RS. The immunologic functions of the neonatal Fc receptor for IgG. J Clin Immunol. 2013; 33(Suppl 1):S9–17. [PubMed: 22948741]

37. Robbins JB, Chu C, Schneerson R. Hypothesis for vaccine development: protective immunity to enteric diseases caused by nontyphoidal salmonellae and shigellae may be conferred by serum IgG antibodies to the O-specific polysaccharide of their lipopolysaccharides. Clin Infect Dis. 1992; 15:346–361. [PubMed: 1381621]

38. Robbins JB, Schneerson R, Szu SC. Perspective: hypothesis: serum IgG antibody is sufficient to confer protection against infectious diseases by inactivating the inoculum. J Infect Dis. 1995; 171:1387–1398. [PubMed: 7769272]

39. Phalipon A, Kaufmann M, Michetti P, Cavaillon JM, Huerre M, Sansonetti P, Kraehenbuhl JP. Monoclonal immunoglobulin A antibody directed against serotype-specific epitope of Shigella flexneri lipopolysaccharide protects against murine experimental shigellosis. J Exp Med. 1995; 182:769–778. [PubMed: 7544397]

40. Klechevsky E, Morita R, Liu M, Cao Y, Coquery S, Thompson-Snipes L, Briere F, Chaussabel D, Zurawski G, Palucka AK, Reiter Y, Banchereau J, Ueno H. Functional specializations of human epidermal Langerhans cells and CD14+ dermal dendritic cells. Immunity. 2008; 29:497–510. [PubMed: 18789730]

41. Way SS, Borczuk AC, Goldberg MB. Thymic independence of adaptive immunity to the intracellular pathogen Shigella flexneri serotype 2a. Infect Immun. 1999; 67:3970–3979. [PubMed: 10417163]

42. Raqib R, Ljungdahl A, Lindberg AA, Andersson U, Andersson J. Local entrapment of interferon gamma in the recovery from *Shigella dysenteriae* type 1 infection. Gut. 1996; 38:328–336. [PubMed: 8675083]

43. Raqib R, Gustafsson A, Andersson J, Bakhiet M. A systemic downregulation of gamma interferon production is associated with acute shigellosis. Infect Immun. 1997; 65:5338–5341. [PubMed: 9393836]

44. Van de Verg LL, Mallett CP, Collins HH, Larsen T, Hammack C, Hale TL. Antibody and cytokine responses in a mouse pulmonary model of Shigella flexneri serotype 2a infection. Infect Immun. 1995; 63:1947–1954. [PubMed: 7729907]

45. Sellge G, Magalhaes JG, Konradt C, Fritz JH, Salgado-Pabon W, Eberl G, Bandeira A, Di Santo JP, Sansonetti PJ, Phalipon A. Th17 cells are the dominant T cell subtype primed by Shigella flexneri mediating protective immunity. J Immunol. 2010; 184:2076–2085. [PubMed: 20089698]

46. Lewis DJ, Huo Z, Barnett S, Kromann I, Giemza R, Galiza E, Woodrow M, Thierry-Carstensen B, Andersen P, Novicki D, Del GG, Rappuoli R. Transient facial nerve paralysis (Bell's palsy) following intranasal delivery of a genetically detoxified mutant of *Escherichia coli* heat labile toxin. PLoS ONE. 2009; 4:e6999. [PubMed: 19756141]

47. Mutsch M, Zhou W, Rhodes P, Bopp M, Chen RT, Linder T, Spyr C, Steffen R. Use of the inactivated intranasal influenza vaccine and the risk of Bell's palsy in Switzerland. N Engl J Med. 2004; 350:896–903. [PubMed: 14985487]

48. Walker RI. Considerations for development of whole cell bacterial vaccines to prevent diarrheal diseases in children in developing countries. Vaccine. 2005; 23:3369–3385. [PubMed: 15837361]

Abbreviations

ASC	antibody secreting cells
BALF	bronchoalveolar lavage fluid
BCG	Bacillus Calmette–Guérin
DC	dendritic cells
DLN	draining lymph node

dmLT	*E. coli* double mutant heat-labile toxin [LT (R192G/L211A)
i.d.	intradermal(ly)
IHC	immunohistochemistry
IF	immunofluorescence
i.n.	intranasal(ly)
LC	Langerhans cells
M_{red}	Mander's overlap coefficient of the red channel
TTSS	type III secretion system

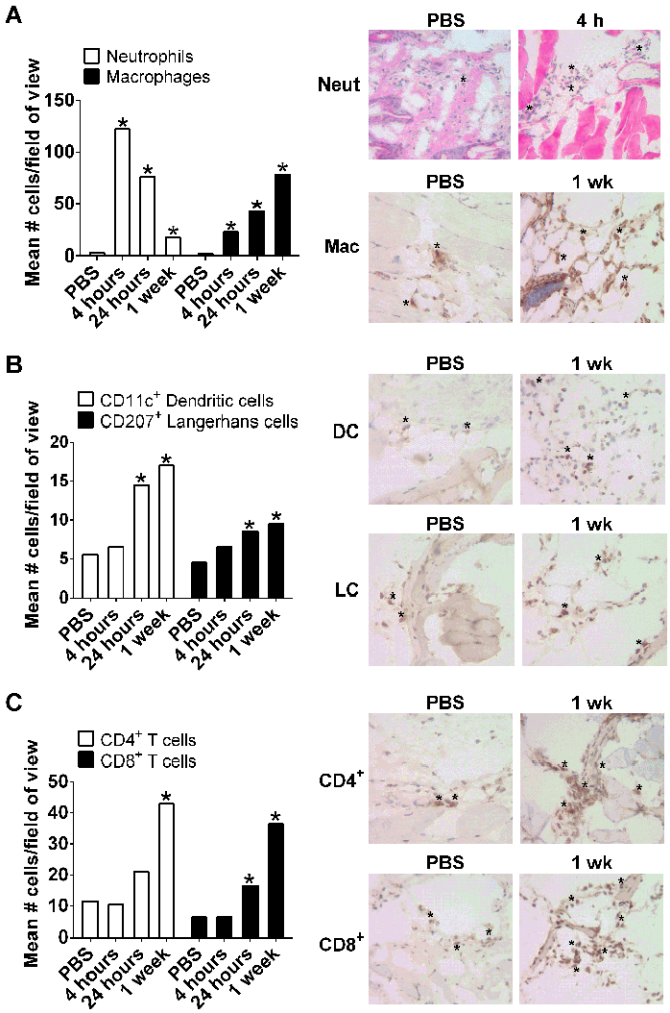

Figure 1.

Immune cells recruited into the skin following i.d. vaccination with IpaB, IpaD and dmLT. Skin sections (bleb region) obtained following i.d. administration of IpaB (100 ng), IpaD (250 ng) and dmLT (100 ng) or PBS were stained by IHC. The number of cells stained positive with Ab recognizing mouse neutrophils (anti-LY-6G), skin macrophages (ER-MP23), DC ($CD11c^+$), LC ($CD207^+$, Langerin) and $CD4^+$ and $CD8^+$ T cells were counted under ×400 magnification in ten representative fields of view. Bars depict the mean cell number per field + SEM for (A) neutrophils and macrophages, (B) DC and LC and (C) $CD4^+$ and $CD8^+$ T cells. The number of neutrophils was determined based on cell morphology in H&E stained slides. In all graphics, the PBS bar denotes mean value across time points. Asterisks on bar graphs (left panels) denote significant differences comparing tissue of immunized mice versus PBS controls, where $p < 0.05$. The right panels show H&E (top row) and IHC images representative of the highest and lowest cell counts; * indicates examples of positive staining used for counting.

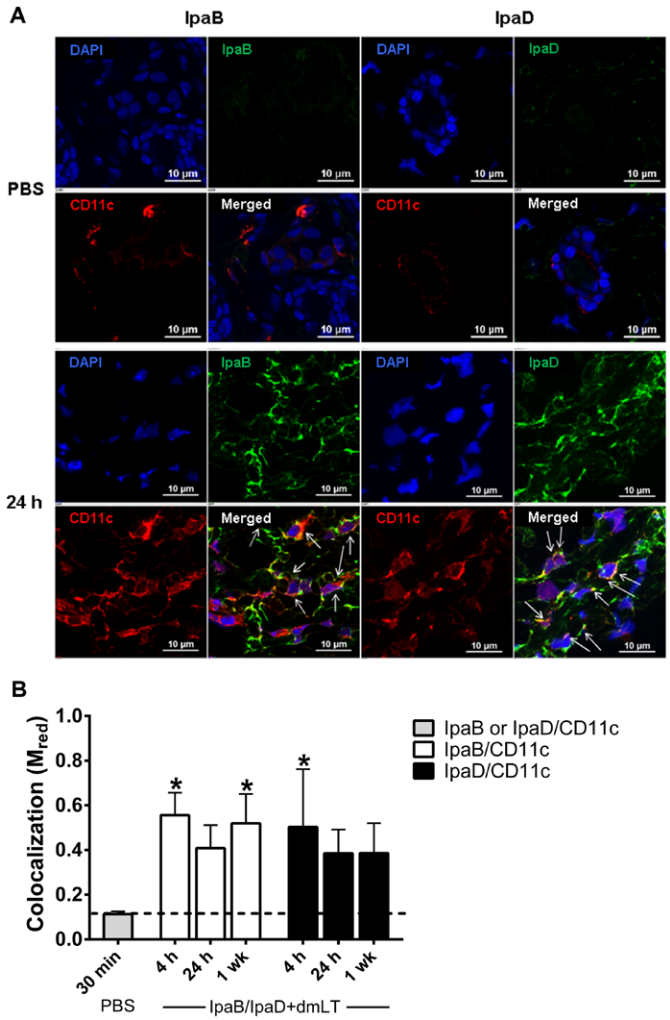

Figure 2.

IpaB and IpaD taken up by skin dendritic cells. (A) Confocal microscopy IF images of skin tissue from mice immunized with IpaB, IpaD and dmLT 24 h following vaccination or from mice that received PBS, 30 min following injection. Sections were stained with mAb specific for IpaB, IpaD (green) or $CD11c^+$ DC (red). The cell nuclei were stained with DAPI (blue). The merged images show all three channels. Arrows on merged images indicate cells with positive staining for antigen (IpaB or IpaD) and CD11c. (B) The graphic shows the extent of colocalization (presented as M_{red}) between IpaB or IpaD (green) with $CD11c^+$ DC (red) at different time points following vaccination. Values represent M_{red} as mean+ SD from 6 z-stack images. The dashed line indicates the baseline level, which corresponds to the mean M_{red} of PBS tissue images. Asterisks denote significant differences between vaccinates versus PBS control mice, where $p < 0.05$.

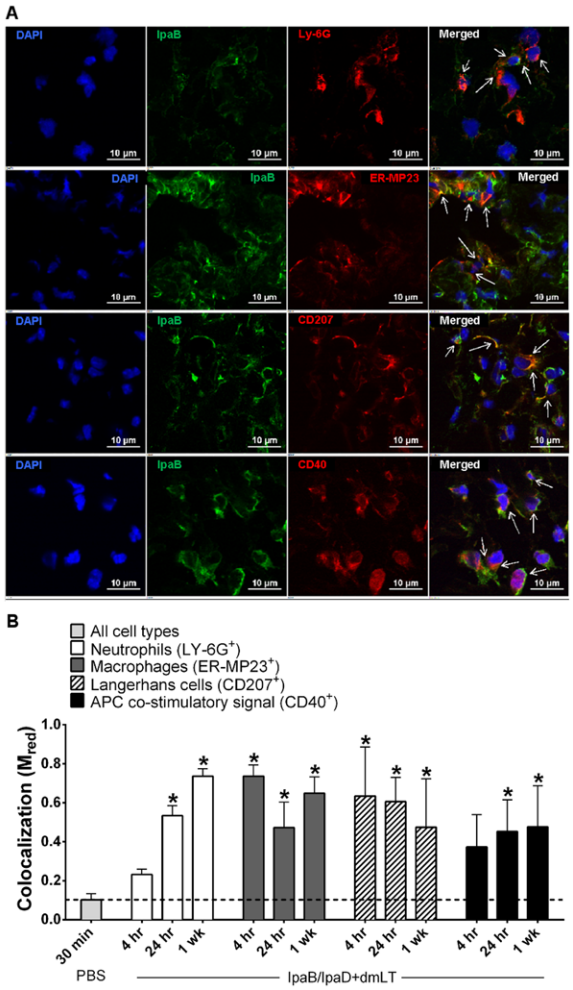

Figure 3.

IpaB sampled by innate immune effector cells in the skin with activated phenotype. (A) Confocal IF images of skin tissue excised 24 h after vaccination show IpaB stained green and neutrophils (LY-6G$^+$), macrophages (ER-MP23$^+$), LC (CD207$^+$, Langerin) or activated APC (CD40$^+$) stained red. (B) The graph shows the extent of colocalization (presented as M_{red}) between IpaB and the indicated cell types at different time points. Values represent M_{red} as mean+ SD from 6 z-stack images. The dashed line indicates the baseline level, which corresponds to the mean M_{red} of PBS tissue images. Asterisks denote significant differences between vaccinates versus PBS control mice, where $p< 0.05$.

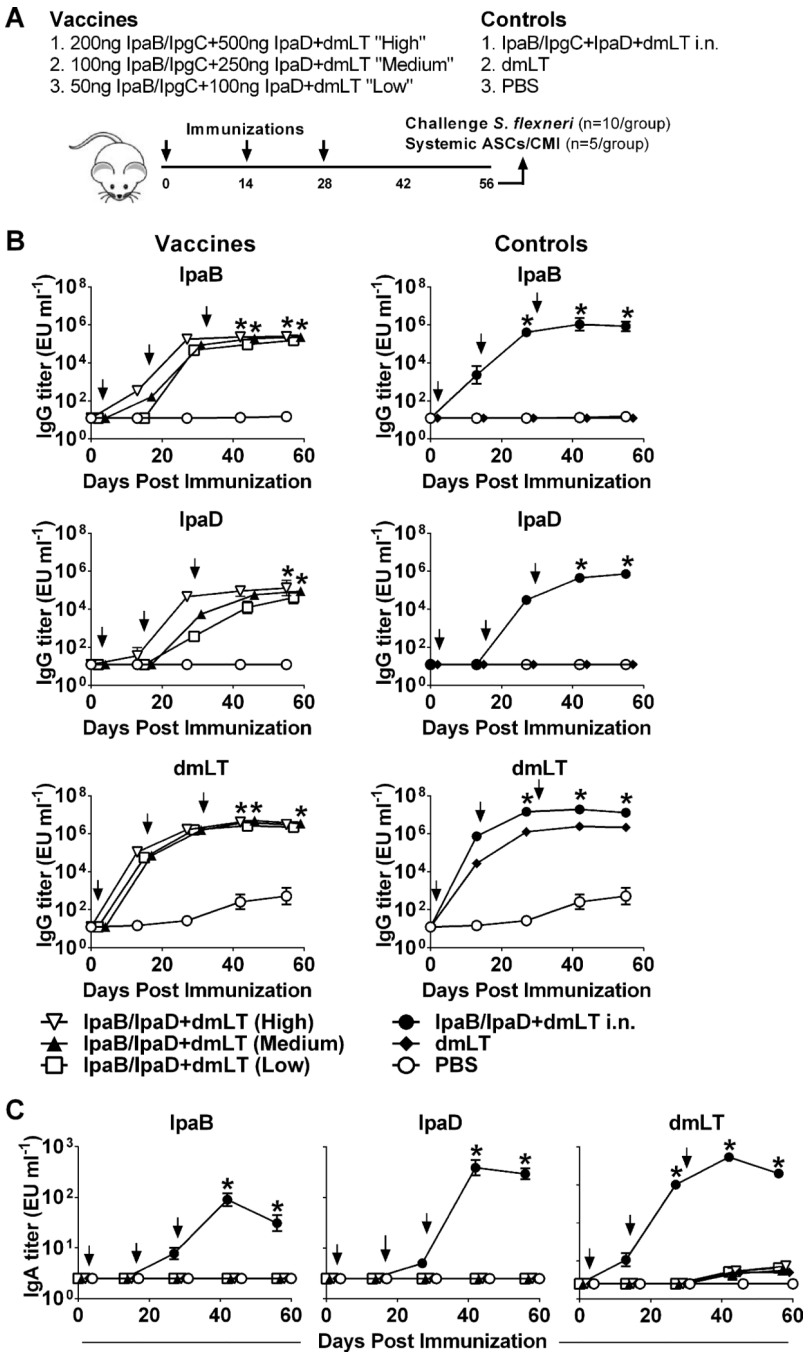

Figure 4.

Serum IgG and fecal IgA responses to vaccine Ag. (A) Mice were immunized i.d. on days 0, 14 and 28 (arrows) with increasing dosage levels of IpaB with IpgC chaperone (IpaB/IpgC) and IpaD, admixed with dmLT. Control groups received IpaB/IpgC, IpaD and dmLT i.n., dmLT alone or PBS. IpaB-, IpaD- and dmLT-specific serum IgG (B) and stool IgA (C). Data represent mean titers ±SEM from 10 individual mice per group. Arrows indicate immunization. Asterisks denote statistically significant differences comparing vaccinated mice versus PBS control, where $p < 0.05$.

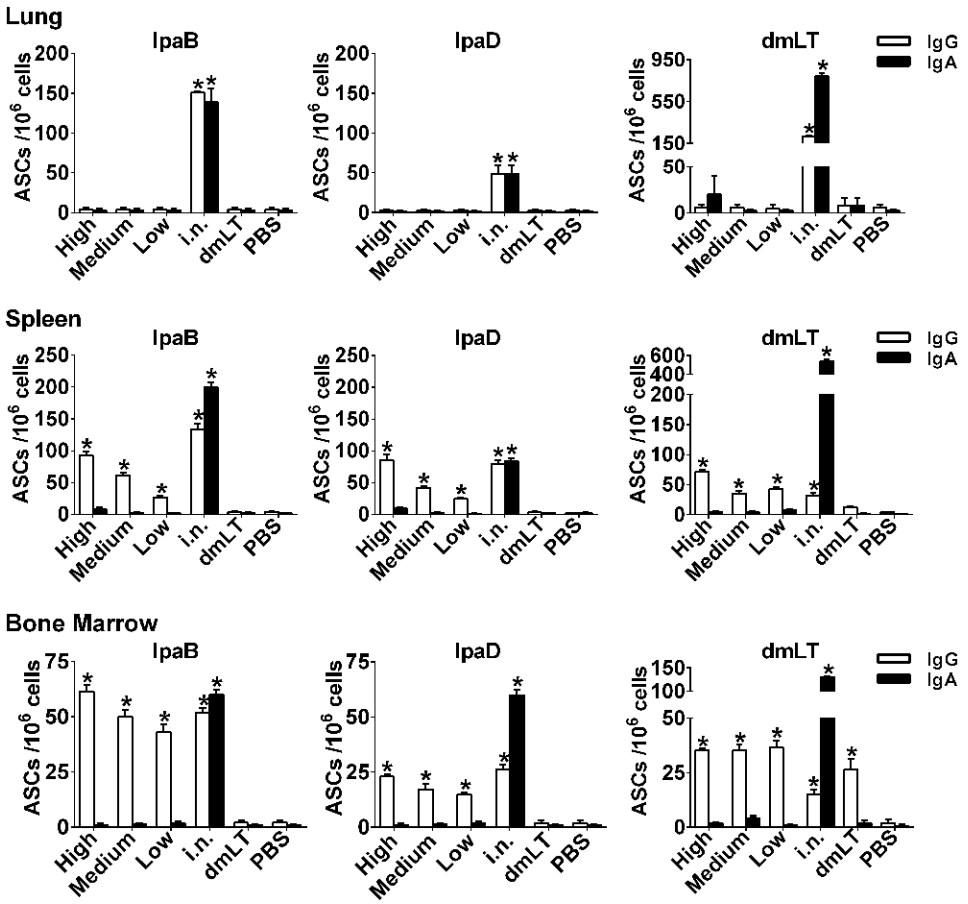

Figure 5.

ASC in mucosal and systemic tissues. Mice were immunized with IpaB, IpaD and dmLT as described in Figure 2A. The frequency of Ag-specific ASC was measured lung, spleen and bone marrow cells obtained on day 56 after vaccination (the time of challenge). The data represent mean ASC counts/10^6 cells+SEM from quadruplicate wells. Asterisks denote significant differences between vaccinated mice versus PBS controls, where $p < 0.05$.

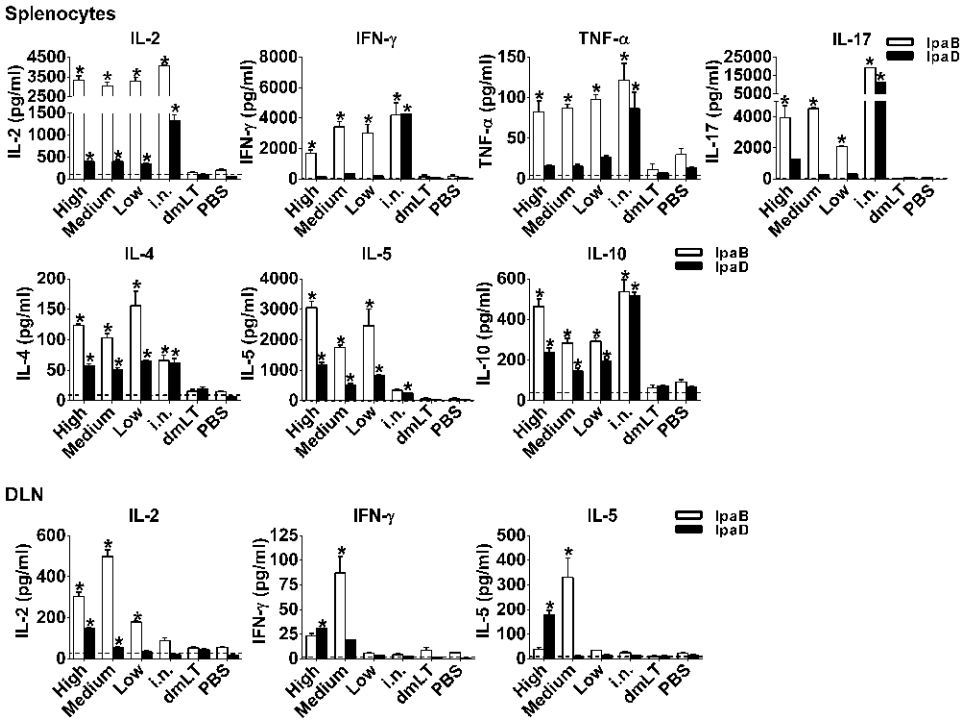

Figure 6.

Cytokines produced by spleen and DLN cells upon IpaD and IpaB stimulation. Mice were immunized with IpaB, IpaD and dmLT as described in Figure 2A. Cytokine levels were measured in culture supernatants from spleen and DLN stimulated in vitro with IpaB and IpaD. Results show mean concentration +SEM from triplicate wells. Dashed line represents average levels produced by un-stimulated cells from vaccinated animals. Asterisks denote significant differences comparing vaccine mice versus PBS groups, where $p < 0.05$.

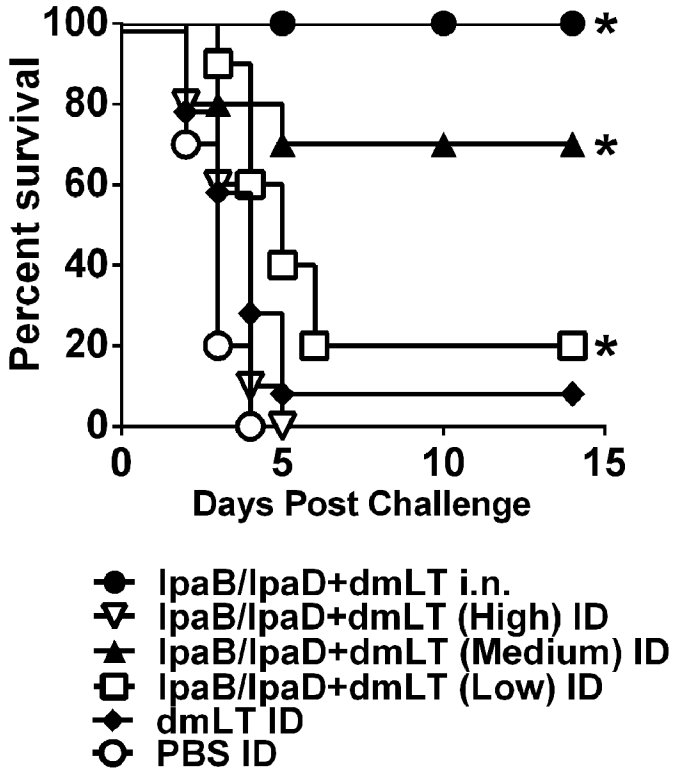

Figure 7.

Protection against *S. flexneri* lethal pulmonary challenge. Mice were immunized as described in Figure 5A and on day 56 they were challenged i.n. with 5.8×10^7 CFU of *S. flexneri* 2a. Data represent survival curves from 10 mice per group. Asterisks indicate significant differences comparing survival curves of vaccine groups versus PBS control, $*p < 0.05$.

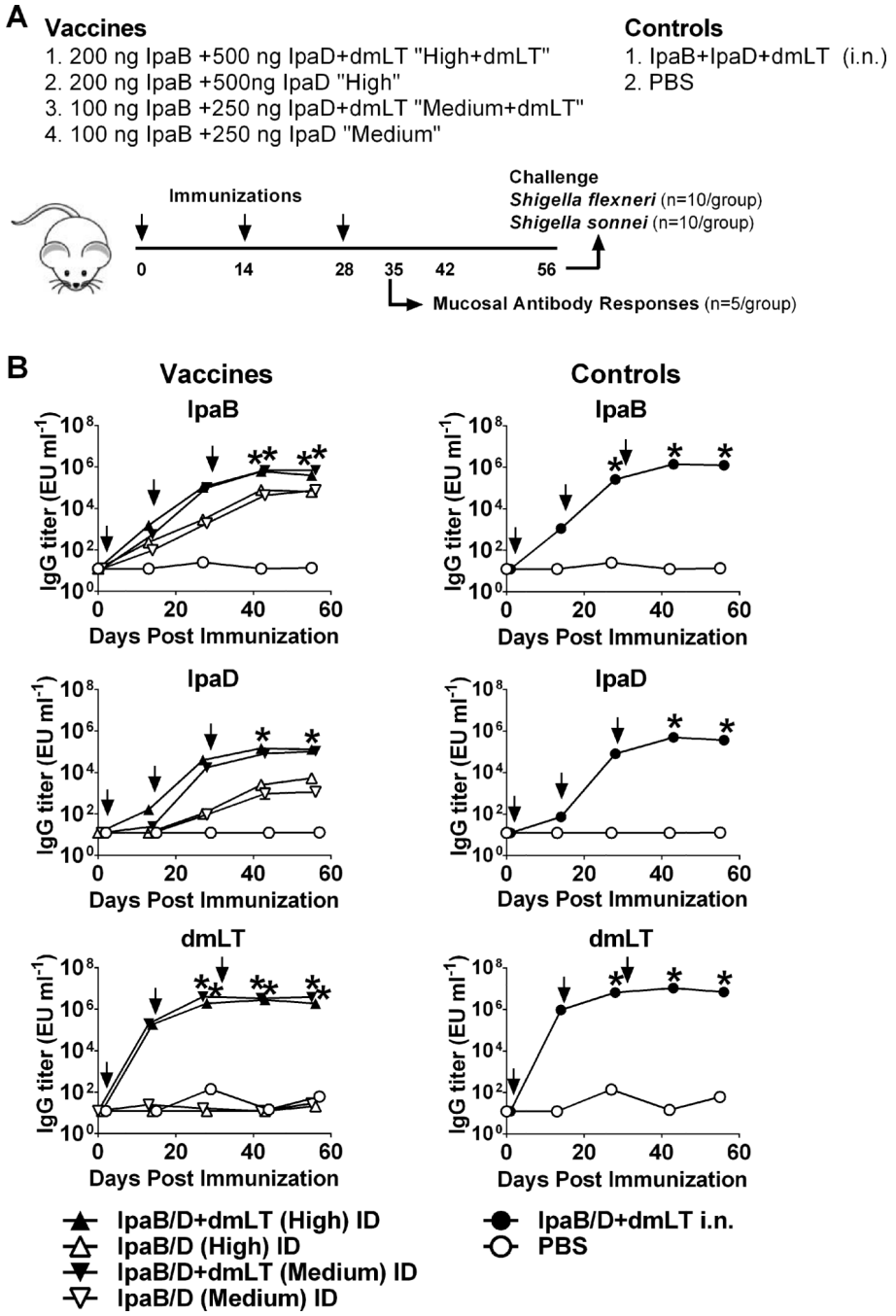

Figure 8.

Serum IpaB-, IpaD-, and dmLT specific IgG responses. (A) Mice were immunized i.d. with IpaB and IpaD at the high and medium doses, with and without dmLT, on days 0, 14, and 28. Controls received IpaB, IpaD, and dmLT i.n. or PBS. (B) IpaB-, IpaD-, and dmLT-specific IgG titers were measured in serum by ELISA. Data represent mean titers ± SEM from 20 mice/group measured on day 55 and 10 mice/group measured at all other time points. Arrows indicate immunization. *$p < 0.05$, vaccine groups versus PBS control.

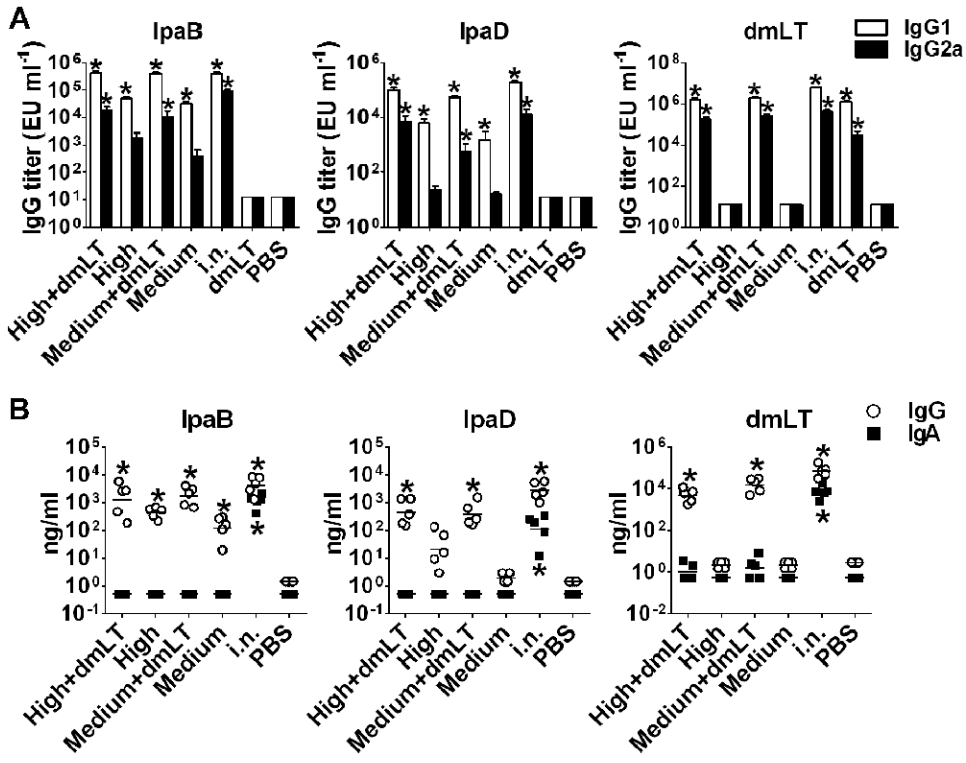

Figure 9.

Serum IgG subclasses and BALF IpaB-, IpaD- and dmLT-specific antibodies. Mice were immunized with high and medium dosage levels of IpaB and IpaD, with or without dmLT as described in Figure 8A. IgG1 and IgG2 were measured on day 56. Subclass responses were also measured in mice that received dmLT alone from Experiment 1 (Figure 5A), as this group was not included in Experiment 2. (A) Data represent mean IpaB-, IpaD- and dmLT-specific IgG1 and IgG2a titers from 10-20 mice per group + SEM. (B) Individual IpaB-, IpaD- and dmLT-specific IgG and IgA titers measured in BALF collected on day 35 from 5 mice per group; lines represent mean values. Asterisks denote significant differences between vaccine and PBS groups, where $p < 0.05$.

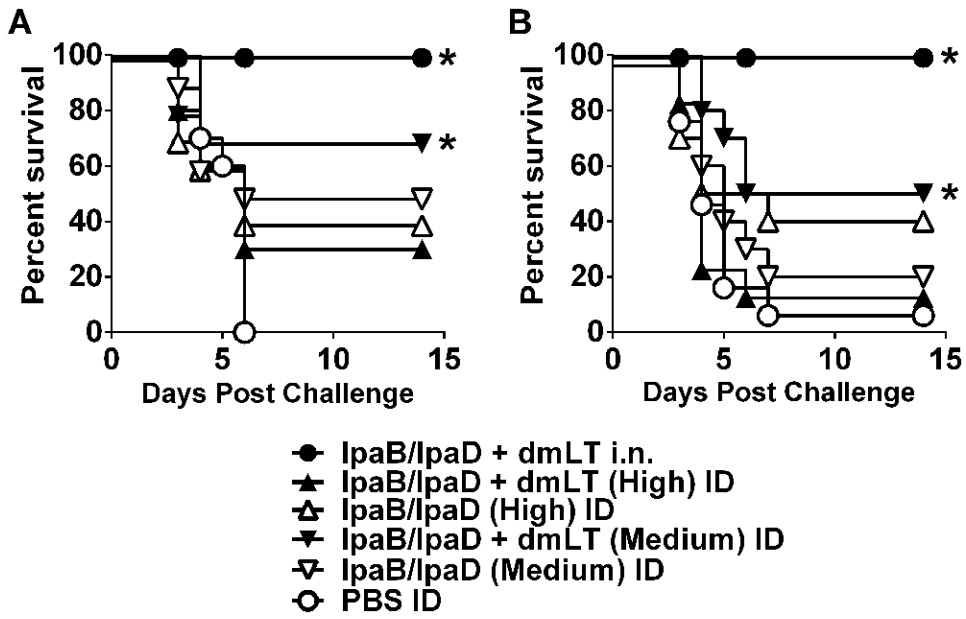

Figure 10.

Protection against *S. flexneri* and *S. sonnei* lethal pulmonary challenge. Mice were immunized as described in Figure 8A and challenged i.n. on day 56 with (A) 5.4×10^7 CFU of *S. flexneri* 2a and (B) 1.4×10^8 CFU *S. sonnei*. Data represent survival curves from 10 mice per group. Asterisks denote significant differences comparing survival curves of vaccinated mice versus PBS controls, where $p < 0.05$.